

N70-23202

**NASA TECHNICAL  
MEMORANDUM**

NASA TM X- 52761

NASA TM X-52761

**CASE FILE  
COPY**

**EXPERIMENTAL VERIFICATION OF EFFECTS OF TURBULENT  
BOUNDARY LAYERS ON CHEMICAL-KINETIC  
MEASUREMENTS IN A SHOCK TUBE**

by F. E. Belles and T. A. Brabbs  
Lewis Research Center  
Cleveland, Ohio

**TECHNICAL PAPER** proposed for presentation at  
**19<sup>th</sup>** Symposium on Combustion sponsored  
by the Combustion Institute  
Salt Lake City, Utah, August 23-29, 1970

**EXPERIMENTAL VERIFICATION OF EFFECTS OF TURBULENT  
BOUNDARY LAYERS ON CHEMICAL-KINETIC  
MEASUREMENTS IN A SHOCK TUBE**

**by F. E. Belles and T. A. Brabbs**

**Lewis Research Center  
Cleveland, Ohio**

**TECHNICAL PAPER proposed for presentation at**

**13<sup>th</sup> Symposium on Combustion sponsored  
by the Combustion Institute  
Salt Lake City, Utah, August 23-29, 1970**

**NATIONAL AERONAUTICS AND SPACE ADMINISTRATION**

EXPERIMENTAL VERIFICATION OF EFFECTS OF TURBULENT BOUNDARY LAYERS  
ON CHEMICAL-KINETIC MEASUREMENTS IN A SHOCK TUBE

by F. E. Belles and T. A. Brabbs

Lewis Research Center  
National Aeronautics and Space Administration  
Cleveland, Ohio

SUMMARY

Experiments were conducted to demonstrate the existence and magnitude of the effects of nonuniform shock-tube flow on kinetic results. Atomic-oxygen concentration was observed in a rich  $H_2/O_2/CO/Ar$  mixture behind incident shocks that produced turbulent boundary-layers and essentially constant shock-front temperatures, at eight initial pressures from 50 to 120 torr. The exponential time-constant for growth of  $[O]$  and the time at which peak concentration occurs are governed by the rate constant for  $H + O_2 \rightarrow OH + O$ . Values of the rate constant were fit to the 120-torr data using two analyses: one incorporating the boundary-layer effects on flow properties and residence time as formulated by Mirels; and the other making the conventional assumption of constant post-shock conditions. Two sets of predictions were then made for the lower-pressure runs and compared with experiment. The comparison showed that the conventional analysis is incorrect; that there is a large error in the rate constant derived from it; and that Mirels' formulas satisfactorily account for the observed results.

INTRODUCTION

Mirels has suggested that flow non-uniformities induced by the boundary layer behind an incident shock may significantly affect shock-tube studies

of chemical kinetics. His discussion<sup>1</sup> of these effects was for the quasi-steady case in which the shock and the contact surface have reached their maximum separation<sup>2,3</sup>. Under these circumstances the temperature, density, and gas residence time are all predicted to increase with distance behind the shock front, even though attenuation of the shock is no longer considered.

Mirels' suggestion has apparently not had a great impact on chemists using shock tubes. There have been only a few published instances in which corrections for changing conditions were mentioned and still fewer in which corrections were applied. And even in the most thorough analysis<sup>4</sup> that has been performed, there were no concurrent experiments to show that the kinetic data actually required correction, nor that Mirels' formulation<sup>1</sup> of boundary-layer effects was a proper basis for making corrections. Thus, it is not surprising that others should hesitate to revise the usual practice of interpreting shock-tube data as if the flow remained uniform.

The present work was done to show that the changing conditions behind shock waves do indeed have a significant effect on kinetic data, and to investigate how well Mirels' description of the flow applies to experiments done in the presence of turbulent boundary layers. The approach was to do a kinetic experiment in reverse: Rather than measure rate data, correct them for boundary-layer effects, and then compare the results with other data which are themselves of uncertain accuracy, we exploited the sensitivity to changing flow conditions of a simple chemical system that is already well understood. A very rich  $H_2/O_2/CO$  mixture, when shocked to a suitable temperature, emits a brief pulse of blue light. The shape and time of occurrence of this pulse are governed almost entirely by a single reaction, the rate

and progress of which are sensitive to changes in temperature, density, and residence time. Therefore, the light pulse serves as a chemical transducer with which to probe the flow properties.

A series of observed light pulses was analyzed with and without consideration of boundary-layer effects. The simplicity of the chemistry made it possible to carry out the two analyses by using in each a different value of the crucial parameter: the rate constant of the dominant reaction. The validity of each method of analysis could then be judged by its success in accounting for the experimental results.

## BACKGROUND

### Boundary-Layer Effects

After the shock and contact surface have reached their maximum separation, the temperature, density, and residence time of the gas all increase behind the shock as they would in a subsonic flow if the cross-sectional area of the passage were increasing. For the case of a turbulent boundary layer, the effective area is given by the following equation<sup>1</sup>

$$(A_x/A) = [1 - (x/l_m)^{0.8}]^{-1} \quad (1)$$

where

$A_x$  effective cross-sectional area of tube

$A$  actual cross-sectional area of tube

$x$  distance behind shock, equal to (laboratory time)  $\times$  (shock velocity)

$l_m$  maximum separation of shock and contact surface.

The value of  $l_m$  depends on the gas mixture and its initial temperature and pressure, the hydraulic diameter of the tube, and the Mach number of the shock, and can be calculated from formulas given in reference 3.

### Chemistry

The intensity of the blue light (CO flame-band radiation) that is emitted when a H<sub>2</sub>/O<sub>2</sub>/CO mixture is shock-heated to sufficiently high temperature is directly proportional to the product of CO and O concentrations<sup>5</sup>. If the mixture contains relatively large amounts of H<sub>2</sub> and CO compared to O<sub>2</sub>, very little of the CO is consumed; thus, the light intensity essentially varies with the O concentration, [O].

Well-confirmed theory<sup>6-8</sup> shows that [O] is governed by the following sequence of reactions. Immediately after the gas has been shock-heated, one or both of the following initiation reactions produce a small concentration of chain-carriers (H, O, or OH):



The brief initiation period is followed by an induction period during which the concentrations of all three chain carriers grow exponentially with time and all with the same exponential time constant,  $\alpha$ , as a result of the chain-branching reactions of hydrogen combustion<sup>6</sup>. Various of these reactions assume different degrees of importance in different mixtures but in very rich ones such as that used in the present work (H<sub>2</sub>/O<sub>2</sub> = 10/1),  $\alpha$  is governed almost entirely by reaction (ii) of the H<sub>2</sub> - O<sub>2</sub> combustion mechanism:



In the limit of extreme H<sub>2</sub>/O<sub>2</sub> ratios and in the absence of boundary-layer effects,  $\alpha$  is given by the following equation<sup>6</sup>:

$$\alpha = 2\rho_{21} k_2 [\text{O}_2] \quad (2)$$

where

$\alpha$  exponential time constant for growth of O concentration in laboratory time-coordinate system

$P_{21}$  density ratio across the shock

$k_2$  rate constant for reaction (II)

$[O_2]$  oxygen concentration

The short supply of oxygen in very rich mixtures eventually causes the exponential buildup of  $[O]$  to be offset by rapid depletion<sup>8</sup>. As a result, flame-band radiation is observed to peak and then to drop rapidly. The time at which the peak occurs,  $\tau$ , is also governed mainly by the rate of reaction (II) in the limit of extreme  $H_2/O_2$  ratios, although there is a minor effect of the rate of initiation by reaction (i) as well. This can be seen from the following equation, which is derivable from relations given in references 6 and 8:

$$\tau = \left( \frac{1}{2P_{21}k_2 [O_2]} \right) \ln \left( \frac{2CP_{21}k_2}{k_i} \right) \quad (3)$$

where

$\tau$  time at which peak O concentration occurs in laboratory time - coordinate system

$k_i$  rate constant for reaction (i)

C expression containing factors that remain constant in this experiment.

Despite the small proportion of  $O_2$  present in the extremely rich mixtures under consideration, both the exponential rise and the peak in  $[O]$  occur before any appreciable amount of it has been consumed.

## APPROACH

### Experimental Conditions

The experimental objective was to obtain a set of measurements of  $\kappa$  and  $\tau$  that would, when analyzed with and without consideration of effects induced by a turbulent boundary layer, reveal the presence of such effects. In order to accomplish this, several requirements had to be considered in planning the experiments. These requirements are listed below, together with the measures taken to fulfill them.

Simple chemistry: To avoid the ambiguities that arise when experiments must be analyzed by permuting the rate constants of many reactions. Although Eqs. (2) and (3) are not quantitatively correct for a  $H_2/O_2 = 10/1$  mixture, they do correctly show that  $k_2$  is the only adjustable parameter of any consequence.

Low oxygen concentration: To prevent excessive heat release that might cause irregular waves<sup>9</sup>. The mixture chosen was  $H_2/O_2/CO/Ar = 5/0.5/6/88.5$ . Not the slightest evidence of irregular waves was found, either in light-emission or pressure records.

Low temperature: To keep  $k_2$  low and thereby delay the light pulse so that the boundary layer could exert significant effects (see Eq. (1)). However, the temperature must not be too low lest chain-breaking by  $H + O_2 + M \rightarrow HO_2 + M$  assume undue importance.

Constant temperature: To make pressure the only experimental variable and to eliminate arguments about the influence of the activation energy chosen for (11). By trial-and-error changes in driver pressure, shock-front temperatures were held to the narrow and suitably low range of  $1140^\circ \pm 12^\circ K$ .

High pressure: To assure turbulent boundary layers<sup>3</sup>. The lowest initial pressure used was 50 torr. Runs were made at 10-torr intervals up to 120 torr.

### Analysis

After the oscilloscope records of light intensity had been plotted semi-logarithmically against laboratory time to yield values of  $\mathcal{L}$  and  $\tau$ , the data were analyzed by means of a computer program. This program integrated the equations of chemical change for reactions occurring behind a shock wave and was equipped to handle two cases: (1) the case in which the apparent area of the tube varies under the influence of the boundary layer in accordance with Eq. (1), with resulting changes in temperature, density, and residence time of the gas; and (2) the conventionally-assumed case in which the area remains constant and the only changes in properties are those due to chemical reaction. The two approaches will be referred to subsequently as the varying-area and the constant-area methods of analysis, respectively.

The procedure was as follows. First, the run at the highest initial pressure (120 torr) was analyzed by both methods. By trial-and-error calculations, two different values of  $k_2$  were found that would closely reproduce the observed  $\mathcal{L}$ . Although the chemistry is dominated by reaction 11, 12 other initiation ((i) and (ii)), chain-branching, and recombination reactions pertinent to the  $H_2-O_2-CO$  system were included in the analysis. Values for their rate constants were taken from recent literature and were identical for both methods of calculation.

Next, the calculated peak times were matched to the  $\tau$  observed in the 120-torr run by modifying  $k_i$  (see Eq. (3)). This resulted in two different

values of  $k_i$  corresponding to the two methods of analysis.

The rate constants obtained in this way were as follows:

$$k_2(\text{constant area}) = 2.10 \times 10^{14} \exp(-16600/RT) \quad (4a)$$

$$k_2(\text{varying area}) = 1.44 \times 10^{14} \exp(-16600/RT) \quad (4b)$$

$$k_i(\text{constant area}) = 2.10 \times 10^{12} \exp(-39000/RT) \quad (5a)$$

$$k_i(\text{varying area}) = 1.20 \times 10^{12} \exp(-39000/RT) \quad (5b)$$

Only the pre-exponential parts of Eqs. (4) and (5) resulted from the trial-and-error fits; the activation energies were assigned. That for reaction (II) was derived from an Arrhenius plot, covering a wide temperature range, of rate constants from many literature sources that were considered reliable. The activation energy assigned to reaction (i) is the value reported in reference 10.

The final step in the analysis was to use the two sets of rate constants to predict constant- and varying-area values of  $\alpha$  and  $\tau$  for the runs made at the pressures below 120 torr. Comparison of the predictions with the experimental data could then be made.

## APPARATUS AND PROCEDURE

### Shock Tube

The tube was a single piece of stainless steel, 5.7 meters long. The internal dimensions were 6.4 x 6.4 cm. with corners rounded to a radius of 1.3 cm. The entire length of the tube was ground to constant inside dimensions and then honed to a highly-polished finish.

Stations for shock-wave detectors were located at 15-cm. intervals in the downstream portion of the tube. A piezoelectric pickup which triggered a raster oscilloscope was followed by four matched pressure transducers

for velocity measurements. These transducers were of the quartz piezoelectric type and had short rise times.

Midway between the last two stations was a pair of 2.5-cm. diameter windows made of calcium fluoride and located opposite one another. A thin-film gauge was located to provide an accurate indication of the time at which a shock wave arrived at the center of the windows and to ascertain that the boundary layer was turbulent. All pickups and windows were carefully installed with their surfaces flush with the inner walls of the tube.

The assembled tube could be evacuated to a pressure of about 1 micron and had a leak rate less than 0.2 micron/minute. A liquid nitrogen cold trap in the vacuum line guarded against the possible back-migration of pump oil.

#### Velocity Measurement

The overriding experimental requirement was the precise measurement of shock velocity. Uncertainties as large as 1 percent, frequently tolerated in shock-tube work, would have completely vitiated the results of this particular experiment. This can be seen by examining Fig. 1. These computed profiles of the product of CO and O concentrations are equivalent to light-emission histories. The differences in shape and peak time are readily apparent.

The required precision was obtained by electronically processing the signals from the four matched transducers so as to produce pulses. These were displayed on a raster oscilloscope along with 1-microsecond timing marks. In this way, velocities were measured with an uncertainty of 0.2 percent.

### Light-Detection System

Flame-band emission was observed through one of the windows by means of a 1:1 optical transfer system. A lens imaged the center of the shock tube onto a slit, 0.25 mm wide, which acted as a field stop. The illuminated slit became the light source for a spherical mirror, which transferred the luminous image at unit magnification through a filter (bandpass, 3700-5600 Å) and onto the cathode of a photomultiplier tube. The rise-time of the photomultiplier, complete with load resistor and cabling, was checked by a gallium phosphide photo-diode that was driven by a square-wave generator. The 1/e rise time was close to 1 microsecond.

### Gas Mixture

The test mixture was prepared by the method of partial pressures in a stainless-steel tank. Oxygen and hydrogen were research grade gases. Carbon monoxide was CP grade and was cold-trapped to remove carbonyls. Argon had a stated purity of 99.99 percent and was cold-trapped to eliminate water vapor. After preparation, the mixture was allowed to stand for a week to insure homogeneity.

## RESULTS AND DISCUSSION

### Experimental Data

Figure 2 shows the oscilloscope record obtained for the run at 90 torr initial pressure. The clean, noise-free character of this record is completely typical of all the data. After arrival of the shock wave at the observation point, indicated by the deflection of the middle trace, no light was observed for some time. Then, a brief and almost symmetrical pulse of

flame-band radiation appeared, reflecting the anticipated rise and fall of atomic-oxygen concentration. The lower trace shows the thin-film signal at higher gain; the continuous rise following the initial jump shows that the boundary layer was thoroughly turbulent, as desired. Had there been any appreciable laminar portion, it would have shown up as a horizontal line following the initial jump<sup>11</sup>.

As stated earlier, the two experimentally observable properties to be used in the evaluation of boundary-layer effects were the exponential time constant,  $\mathcal{L}$ , and the peak-time,  $\mathcal{T}$ , of the atomic oxygen concentration. These were obtained from semi-logarithmic plots of light intensity against laboratory time. Figure 3 is such a plot, made from data read off the original of Fig. 2. The well-defined exponential part of the record comprised 1.5 to 2 decades of rising light intensity in all runs. The slope,  $\mathcal{L}$ , of a line drawn by eye through this linear portion of Fig. 3 and the peak-time,  $\mathcal{T}$ , also picked off visually, are given in Table I together with the results of the runs at the other pressures.

#### Analytical Data

In addition to experimental results, Table I contains the following calculated data.

Shock-front temperatures were computed from the shock velocity measured by the two pickups straddling the window. This computation employed a machine program in which full thermal equilibrium was assumed, real-gas thermodynamic data were used, and chemical composition was assumed frozen. Other results of the shock calculation, while not listed, were needed as inputs for the analysis; these included the pressure, density, and velocity of the shocked gas.

As already described in the section on Analysis, the two methods of treating experimental data were applied to the 120-torr run to obtain two sets of rate constants that gave close fits to the observed  $\alpha$  and  $\tau$ . These rate constants were then used to obtain the predicted constant-area and varying-area values of  $\alpha$  and  $\tau$  that are listed for each run at the lower pressures.

The values of  $l_m$ , needed to define the apparent area change in the varying-area analysis, were calculated by formulas<sup>3</sup> that apply to the case of all-turbulent boundary layers. This calculation required the use of a quantity, designated  $\beta_0$  in reference 3, which is tabulated there for argon and for air. Inasmuch as the mixture contained 88.5 percent argon, the value of  $\beta_0$  for that gas was used.

#### Comparison of Analyses

The two methods of analysis are most readily compared in terms of the ratios of predicted to observed values of  $\alpha$  and  $\tau$ . Barring experimental errors, a completely successful analysis should produce values of these ratios that are as close to unity for the lower-pressure runs as they are for the 120-torr run.

Figure 4 shows the results. It is immediately evident that the varying-area analysis based on Eq. (1) is superior to the conventional one in which boundary-layer effects are neglected. The constant-area method introduces a discrepancy with experiment that increases as pressure decreases from the match point at 120 torr.

This pressure effect can be understood by considering Fig. 5. Here the computed effects of the boundary layer are shown for the 90-torr run, which is typical of the others in this respect. At low pressure, where the reaction rate is reduced and the light pulse tends to be delayed and spread out, there is a counteracting effect due to the rising residence time and rate constant. Hence,  $\mathcal{L}$  and  $\tau$  do not change with pressure as much as they would in the absence of flow non-uniformities.

It should be noted that the effects plotted in Fig. 5 are gas-dynamic and not due to any peculiarity of the chemistry that is involved in this particular experiment. Virtually identical curves result if the calculations are repeated with all rate constants set equal to zero.

#### Shock-Contact Surface Separation

The success of the varying-area analysis in accounting for the experimental results suggests that the essential ingredient in the analysis,  $l_m$ , should be examined more closely. Although the immediate aim of this work was to exhibit the effects of flow non-uniformities in a kinetic experiment and to ascertain that Mirels' approach could deal with them, the ultimate use of the results should be to improve the accuracy of shock-tube kinetic data. In this latter regard, the use of calculated  $l_m$ 's (calculated, moreover, using values of  $\beta_0$  for pure argon) introduces an element of uncertainty. It was therefore decided to measure the lengths.

This was done by setting up an infrared monochromator with an indium antimonide detector coupled to an oscilloscope, to observe 4.7-micron emission from CO in the gas mixture. Runs were made at 50, 70, 90, and

120 torr, over the same small range of shock velocities as before. A sharp jump in emission corresponded to the arrival of the shock at the window and an abrupt drop to the arrival of the contact surface. The measured separation length,  $l$ , was obtained by multiplying the duration of infrared emission by the shock velocity.

The measured  $l$ 's were within 20 percent of the  $l_m$ 's calculated for the same pressures. Thus, it is clear why the varying-area analysis succeeded so well. Nevertheless, the experiments were re-analyzed using  $l$ 's read from a line faired through a plot of  $l$  against initial pressure (see Table II). The same rate constants (Eqs. 4(b) and 5(b)) were used. The results, listed in Table II as ratios of predicted to observed values of  $\alpha$  and  $\tau$ , show by comparison with corresponding data based on  $l_m$  that use of the measured  $l$ 's improves the agreement in  $\alpha$  and leaves  $\tau$  virtually unchanged.

Also in Table II are results showing the consequences of applying the theory<sup>3</sup> of separation-length development, according to which calculation  $l$ 's should have been much less than  $l_m$  at the window position of the shock tube. Re-analysis with these predicted separations required re-fitting the 120-torr run; this yielded a new  $k_2$  15 percent smaller than before. The results at the lower pressures (Table II) are clearly inferior to those obtained with measured  $l$ 's.

Whether the unexpectedly rapid approach to  $l_m$  is a general rule or peculiar to this tube is unclear. Until the situation is clarified, it will be necessary to use measured separations in the reduction of shock-tube data.

### Implications for Shock-Tube Kinetics

The experimental results obtained in this experiment can be viewed as data designed to determine the rate constant to which the results are most sensitive, namely,  $k_2$ . From this point of view, the effect of applying boundary-layer corrections is two-fold. First, the rate constant at 120 torr is 30 percent less than the value obtained when corrections are neglected; and second, repeat determinations at lower pressures yield values with an average error of only  $\pm 4.3$  percent, while the conventional treatment of the data produces a pressure-dependent rate constant.

This suggests that much of the shock-tube kinetic data in the literature is wrong in some degree. It is also likely that some of the scatter and some of the discrepancies in the results of different investigators, commonly noted in shock-tube work, can be attributed to the neglect of boundary-layer effects. Consider, for example, what would have happened if only the runs at 50 and 120 torr had been made and analyzed in the usual way. Assuming that the activation energy were known so as to take account of the difference in shock-front temperatures, the result would have been two values of the pre-exponential part of  $k_2$  that differed by 25 percent. This would no doubt have been accepted as experimental scatter. It is apparent that an even larger difference could have been found if these two runs had been made in separate shock tubes, especially if the tubes differed in length and diameter.

The size and the sign of the errors in existing data depend in a complicated way on the size of the tube, the position of the observation point,

the gas mixture and pressure used, and the type of measurements made, as well as on the rate and activation energy of the reaction. Rate constants derived from measurements close to the shock front are obviously the least suspect. Thus, the results of an investigation that covered a temperature range are likely to be more reliable at the high end of the range. At the low end, where rates are low and observations must be extended far behind the shock, large errors are possible, especially if the activation energy is large and therefore causes the rate to grow rapidly because of the rising temperature during the observation period. Although the error incurred by neglecting the flow non-uniformities in such an experiment may be either positive or negative, in most cases it will be positive (Ref. 4 describes a less-common case in which the error was negative). Therefore, a general tendency must exist in the literature for low-temperature rate constants to be too large, while high-temperature values are more nearly correct, so that activation energies will tend to be too low. An example of this behavior is the activation energy of (11), which was found to be 16.3 kcal/mole with and only 11.9 kcal/mole without corrections for nonuniform flow<sup>12</sup>.

#### CONCLUSIONS

Changes in temperature, density, and residence time induced by turbulent boundary layers in shock tubes have been shown by careful experiments on a simple chemical system to significantly affect both the accuracy and reproducibility of kinetic results. Existing boundary-layer theory, together with measured separations between shock and contact surface, satisfactorily accounts for these effects. The results show that much of the existing data based on the conventional assumption of uniform flow must, in varying degrees, contain some error.

REFERENCES

1. MIRELS, H.: Phys. Fluids 9, 1907 (1966).
2. MIRELS, H.: Phys. Fluids 6, 1201 (1963).
3. MIRELS, H.: AIAA J. 2, 84 (1964).
4. WARSHAY, M.: Effects of Boundary Layer Buildup in Shock Tubes Upon Chemical Rate Measurements, NASA TN D-4795, 1968.
5. CLYNE, M. A. A., AND THRUSH, B. A.: Proc. Roy. Soc. (London) A269, 404 (1962).
6. BROKAW, R. S.: Tenth Symposium (International) on Combustion, p. 269, The Combustion Institute, 1965.
7. BROKAW, R. S.: Eleventh Symposium (International) on Combustion, p. 1063, The Combustion Institute, 1967.
8. HAMILTON, C. W., AND SCHOTT, G. L.: Eleventh Symposium (International) on Combustion, p. 635, The Combustion Institute, 1967.
9. SCHOTT, G. L.: Detonation Spin in Driven Shock Waves in a Dilute Exothermic Mixture, Preprints, Am. Chem. Soc. Div. of Fuel Chem., 11, 29, Chicago, Ill., 1967.
10. RIPLEY, D. R., AND GARDINER, W. C., JR.: J. Chem. Phys. 44, 2285, (1966).
11. BROMBERG, R.: Jet Propulsion 26, 737 (1956).
12. BRABBS, T. A., BELLES, F. E., AND BROKAW, R. S.: Thirteenth Symposium (International) on Combustion, p. , The Combustion Institute, 1971.

TABLE 1. - OBSERVED AND PREDICTED EXPONENTIAL TIME CONSTANTS AND PEAK TIMES

Initial pressure, torr	120	110	100	90	80	70	60	50
Shock velocity, mm/ $\mu$ sec	1.042	1.045	1.047	1.050	1.052	1.042	1.045	1.064
Shock-front temperature, $^{\circ}$ K	1128	1133	1136	1141	1144	1128	1133	1152
Limiting separation, $l_m$ , cm	151.0	147.7	144.2	140.5	136.4	131.9	127.0	121.3
Exponential time constant, $\tau \times 10^{-4}$ , sec $^{-1}$ (laboratory time scale)								
Observed	6.77	6.37	6.53	5.67	5.37	4.83	4.69	4.65
Predicted, varying area	6.66 <sup>a</sup>	6.40	6.35	6.22	5.97	5.17	4.93	5.03
Predicted, constant area	6.58 <sup>a</sup>	6.31	5.89	5.63	5.19	4.04	3.69	3.54
Peak time, $\tau$ , $\mu$ sec (laboratory time)								
Observed	193	206	205	226	233	270	311	293
Predicted, varying area	199 <sup>a</sup>	203	211	219	230	274	297	289
Predicted, constant area	187 <sup>a</sup>	194	207	219	238	306	340	345

<sup>a</sup>Fitted by trial-and-error changes in  $k_2$

TABLE 11. - COMPARISON OF VARYING-AREA ANALYSES USING DIFFERENT  
SHOCK-CONTACT SURFACE SEPARATIONS

	Initial pressure, torr								Av. deviation from unity
	120	110	100	90	80	70	60	50	
Measured separation, $l$ , cm.	144.5	145.8	147.0	147.5	147.4	146.6	145.0	142.3	
$\alpha$ (calc'd.)/ $\alpha$ (obs.)	1.003	1.043	.979	1.093	1.093	1.048	1.023	1.022	.043
$\tau$ (calc'd.)/ $\tau$ (obs.)	1.016	.986	1.038	.974	1.007	1.048	.975	1.027	.025
Limiting separation, $l_m$ , cm.	151.0	147.7	144.2	140.5	136.4	131.9	127.0	121.3	
$\alpha$ (calc'd.)/ $\alpha$ (obs.)	.983	1.003	.973	1.095	1.112	1.069	1.052	1.082	.057
$\tau$ (calc'd.)/ $\tau$ (obs.)	1.032	.987	1.029	.969	.987	1.014	.956	.987	.024
Calc'd. separation at window, $l_w$ , cm.	95.1	94.1	93.0	91.8	90.6	89.4	87.5	85.2	
$\alpha$ (calc'd.)/ $\alpha$ (obs.)	1.002	1.080	1.019	1.158	1.184	1.156	1.153	1.170	.115
$\tau$ (calc'd.)/ $\tau$ (obs.)	1.018	.971	1.010	.947	.961	.981	.900	.949	.040

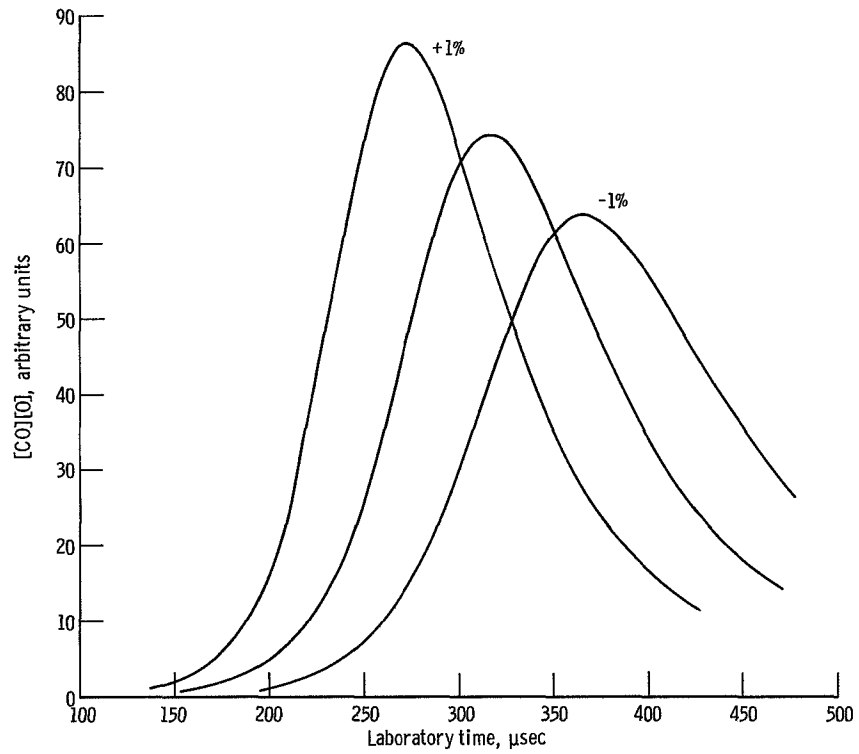


Figure 1. - Illustration of sensitivity of light-emission profile to changes in shock velocity. Calculated by constant-area method for  $H_2/O_2/CO/Ar = 5/0.5/6/88.5$  mixture at 90-torr initial pressure, processed by a shock with velocity required to heat the gas to  $1100^\circ K$  and by shocks 1 percent faster and slower.

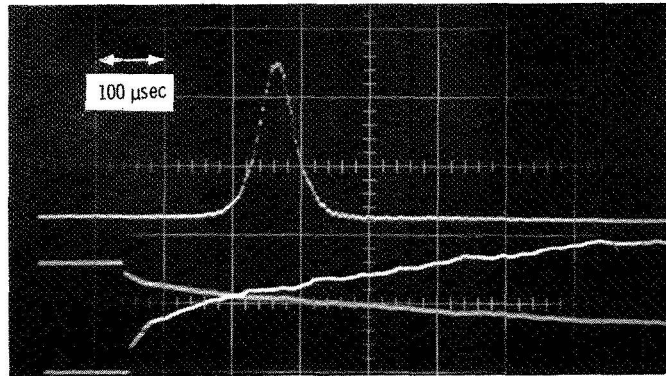


Figure 2. - Experimental record obtained from  $H_2/O_2/CO/Ar = 5/0.5/6/88.5$  mixture at 90-torr initial pressure, shocked to 1141 °K. Upper trace: flame-band radiation. Center trace: thin-film record showing shock arrival at observation point. Lower trace: amplified thin-film record showing immediate onset of turbulent boundary layer.

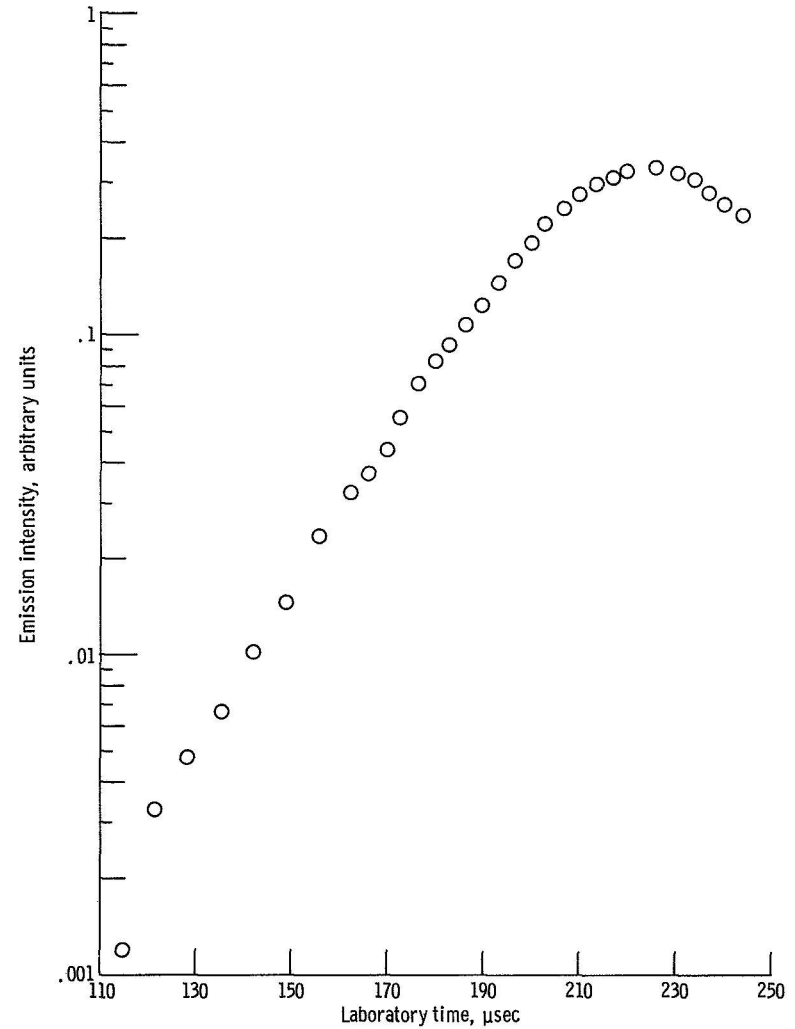


Figure 3. - Semi-logarithmic plot of flame-band emission shown in figure 2.

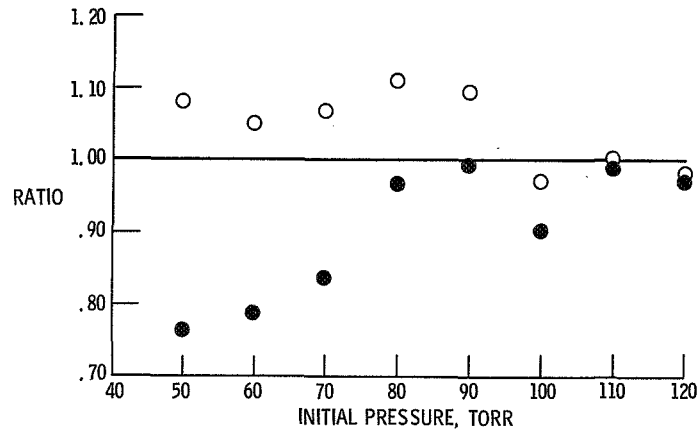


Figure 4(a). - Comparison of predicted and observed exponential time constants.  $\circ$ ,  $\alpha$ (predicted, varying area)/ $\alpha$ (observed).  $\bullet$ ,  $\alpha$ (predicted, constant area)/ $\alpha$ (observed).

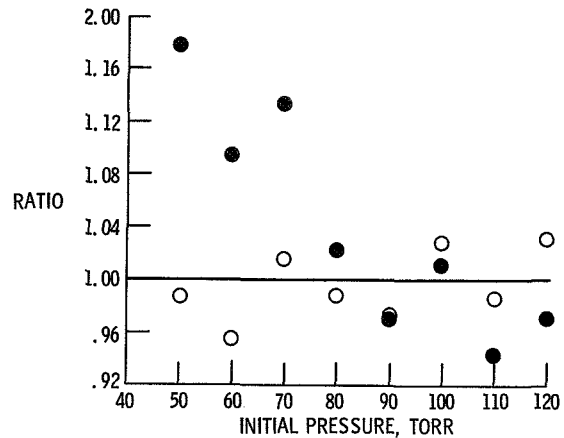


Figure 4(b). - Comparison of predicted and observed peak times.  $\circ$ ,  $\tau$ (predicted varying area)/ $\tau$ (observed).  $\bullet$ ,  $\tau$ (predicted, constant area)/ $\tau$ (observed).

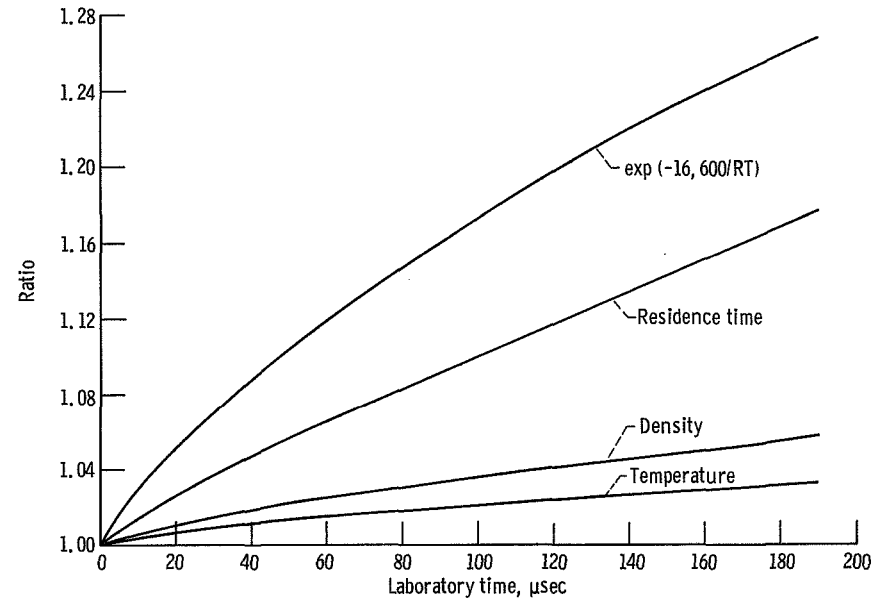


Figure 5. - Variation with time of post-shock properties for 90-torr run shown in figure 2. Ratios of properties calculated by varying-area analysis to those calculated by constant-area analysis.